

## Supplementary Material

### MeT-DB V2.0: Elucidating context-specific functions of N<sup>6</sup>-methyl-adenosine methyltranscriptome

Hui Liu<sup>1,#</sup>, Huaizhi Wang<sup>1,#</sup>, Zhen Wei<sup>2,#</sup>, Songyao Zhang<sup>3,4</sup>, Gang Hua<sup>1</sup>, Shao-Wu Zhang<sup>4</sup>, Lin Zhang<sup>1</sup>, Shou-Jiang Gao<sup>5</sup>, Jia Meng<sup>2,\*</sup>, Xing Chen<sup>1,\*</sup>, and Yufei Huang<sup>3,6,\*</sup>

<sup>1</sup> School of Information and Control Engineering, China University of Mining and Technology, Xuzhou, Jiangsu 221116, China

<sup>2</sup> Department of Biological Sciences, Xi'an Jiaotong-Liverpool University, Suzhou, Jiangsu 215123, China

<sup>3</sup> Department of Electrical and Computer Engineering, the University of Texas at San Antonio, San Antonio, Texas, 78249, USA

<sup>4</sup> Key Laboratory of Information Fusion Technology of Ministry of Education, School of Automation, Northwestern Polytechnical University, Xi'an, 710072, China

<sup>5</sup> Department of Molecular Microbiology and Immunology, Keck School of Medicine, University of Southern California, Los Angeles, CA, 90033, USA

<sup>6</sup> Department of Epidemiology and Biostatistics, the University of Texas Health at San Antonio, San Antonio, Texas, 78229, USA

\* To whom correspondence should be addressed:

Tel: +1-210-4586270; Fax: +1-210-4585947; Email: yufei.huang@utsa.edu (Y.H.)

Correspondence may also be addressed to:

Tel: +86-516-83590818; Email: xingchen@cumt.edu.cn (X.C.)

Tel: +86-512-81880492; Email: jia.meng@xjtlu.edu.cn (J.M.)

#### Table of Contents

Figure S1. The number of MeRIP-seq samples by years

Figure S2. Illustration of m<sup>6</sup>A readers, writers, and erasers in the TREW database

Figure S3. Distribution of MeRIP-seq samples by species and published papers

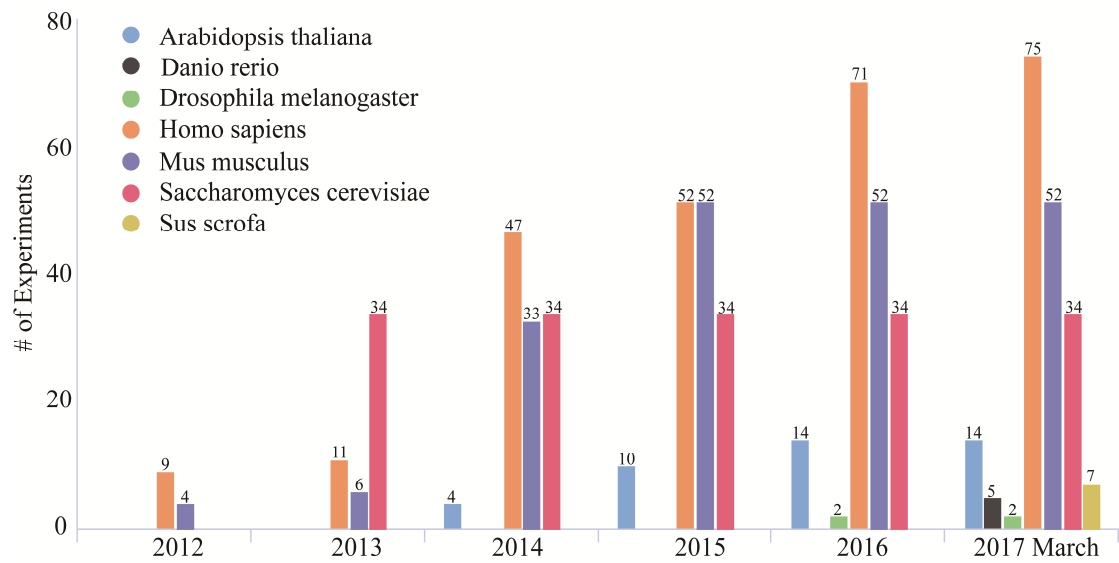
Figure S4. Illustration of table view

Table S1. Studies from which the MeT-DB V2.0 core data samples were obtained

Table S2. Studies from which the TREW data samples were obtained

---

# The authors wish it to be known that, in their opinion, the first 3 authors should be regarded as joint First Authors



**Figure S1. The number of MeRIP-seq samples by years.** Published studies employed MeRIP-Seq experiments grew rapidly, while more and more species were enrolled.

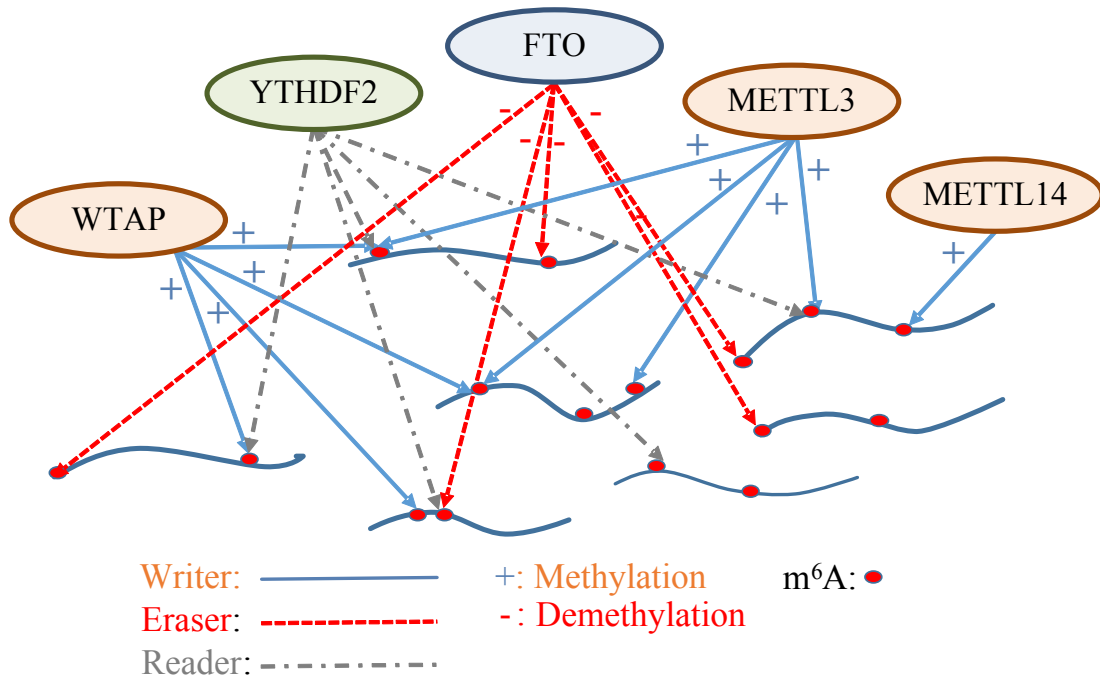


**Figure S2. Illustration of m<sup>6</sup>A readers, writers, and erasers in the TREW database.** TREW is an acronym for the epitranscriptomic Target of Reader, Eraser and Writer. TREW collected ParCLIP-seq and MeRIP-seq samples for 8 regulator/reader proteins (including FTO, KIAA1429, METTL14, METTL3, WTAP, HNRNPC, YTHDC1, YTHDF1) from 10 published studies.

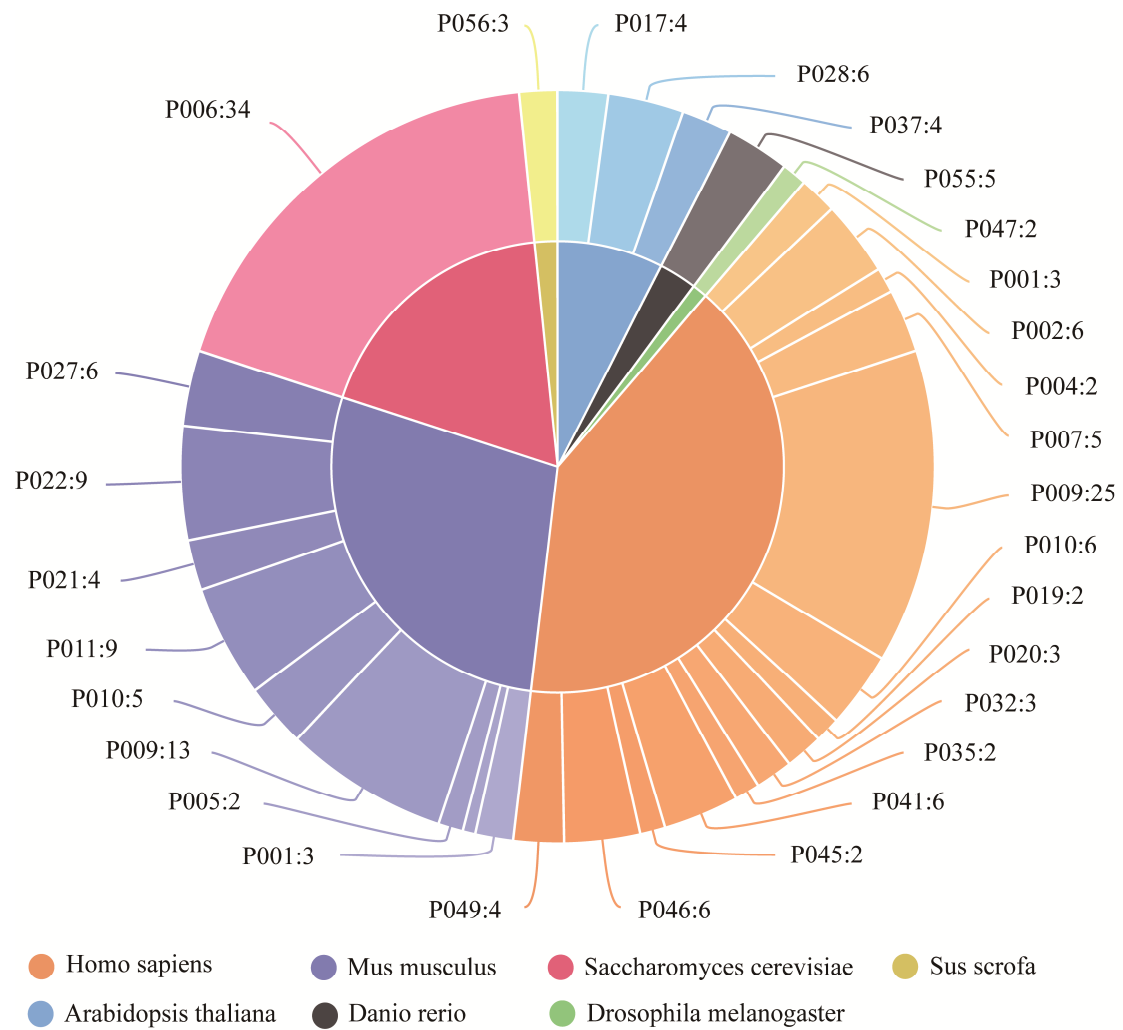


**Figure S3. Distribution of MeRIP-seq samples by species and published papers.** 26 independent studies and 185 MeRIP-Seq experiments were included in MeT-DB V2.0.

**Advanced Functions**

Tools: Export Data Content

Copy | CSV

**Filter SET\_1: Sites Within Genome Region**

Chromosome:  Strand:  Start:  End:

**Filter SET\_2: Sites' Score and Significance**

Fold Enrichment:   P-Value:   FDR:

**Filter SET\_3: Sites Overlapping with Genome Features**

Gene Symbol, Gene ID or RefSeq Accession:  5' UTR:  CDS:  3' UTR:  lncRNA:

**Filter SET\_4: Sites Overlapping with Relative Data**

# HiT mRNA Peaks:   # HiT Single Data mRNAs:   # HiT TREW Sites:   # HiT SNPs:

# HiT miRNA TargetScan Sites:   # HiT miRNA miRanda Sites:   # HiT Splicing Factor:   # HiT RBP:

# HiT Cancer Gene:   # HiT miRtarbase Gene:   # HiT Tumor Suppressor Genes:

Apply Filters | Reset All Filters | Clear Filter Set\_1 | Clear Filter Set\_2 | Clear Filter Set\_3 | Clear Filter Set\_4

**Genomic features**

Search:

show	id	Chrom	ChromStart	ChromEnd	Name	Score	Strand	Pval	Fdr	Fold_enrichment	Gene_name	HiT_mRNA_sites	HiT_SB_mRNA	HiT_TREW	HiT_SNP	HiT_TargetScan	HiT_miRanda	HiT_splicing_factor	HiT_RBP	HiT_CancerGene	HiT_miRtarbase	HiT_TsGene	
	1	chr1	776810	77700	p001_HEK293T_S1_SVSY_1	13	-	0.0001413	0.0007763	12.8	:LINC01128	12	4	0	0	0	0	0	0	0	0	0	0
	2	chr1	777709	778009	p001_HEK293T_S1_SVSY_2	8	+	0.0004467	0.002344	7.96	:LINC01128	26	5	0	0	0	0	0	0	0	0	0	0
	3	chr1	788860	789970	p001_HEK293T_S1_SVSY_3	17	+	5.012e-29	7.943e-28	16.9	:LINC01128	102	32	1	0	0	63	0	0	0	0	0	0
	4	chr1	791688	792468	p001_HEK293T_S1_SVSY_4	28	-	0.000000007244	0.00000006406	27.4	:LINC01128	81	17	1	0	0	33	0	0	0	0	0	0
	5	chr1	792811	793988	p001_HEK293T_S1_SVSY_5	12	+	0.00009491	0.0003651	12	:LINC01128	24	3	0	0	0	13	0	0	0	0	0	0
	6	chr1	878131	878491	p001_HEK293T_S1_SVSY_6	5	+	3.881e-36	6.31e-34	4.66	:SAMD11	35	4	2	0	0	0	0	20	2	0	0	0
	7	chr1	878452	878941	p001_HEK293T_S1_SVSY_7	5	-	5.012e-95	2.512e-93	4.02	:SAMD11	41	7	1	0	0	21	0	74	2	0	0	0
	8	chr1	948484	948981	p001_HEK293T_S1_SVSY_8	7	+	2.512e-19	2.512e-18	6.65	:ISG15	27	5	3	0	0	0	0	7	2	0	1	0
	9	chr1	990362	991021	p001_HEK293T_S1_SVSY_9	11	-	1.966e-34	3.162e-33	10.1	:AGRN	60	6	2	0	5	26	0	88	7	0	0	0
	10	chr1	1167825	1168996	p001_HEK293T_S1_SVSY_10	9	+	2.512e-44	5.012e-43	8.34	:B3GALT6	73	4	3	0	0	0	0	59	0	0	0	0
	11	chr1	1168934	1169618	p001_HEK293T_S1_SVSY_11	12	+	1e-104	1e-102	11.5	:B3GALT6	74	12	1	0	1	47	0	94	0	0	0	0
	12	chr1	1169825	1170420	p001_HEK293T_S1_SVSY_12	10	+	7.943e-07	2.512e-05	9.8	:B3GALT6	65	13	1	0	0	20	0	30	0	0	0	0
	13	chr1	1248878	1247057	p001_HEK293T_S1_SVSY_13	4	+	1.259e-18	1.259e-17	3.7	:PUSL1	27	4	2	0	0	8	0	30	0	0	0	0
	14	chr1	1263031	1263476	p001_HEK293T_S1_SVSY_14	10	+	5.012e-36	7.043e-34	9.46	:CPTP	61	5	3	0	0	7	0	14	4	0	0	0
	15	chr1	1263564	1264276	p001_HEK293T_S1_SVSY_15	8	-	0.31e-27	7.943e-26	7.25	:CPTP	64	14	2	0	0	18	0	62	4	0	0	0
	16	chr1	1335943	1336834	p001_HEK293T_S1_SVSY_16	14	+	1e-154	1e-152	13.7	:LOC148413	74	15	3	0	0	187	0	36	0	0	0	0
	17	chr1	1337150	1337426	p001_HEK293T_S1_SVSY_17	6	-	5.012e-36	7.043e-35	4.40	:LOC148413	45	6	1	0	0	32	0	21	0	0	0	0
	18	chr1	1374529	1374789	p001_HEK293T_S1_SVSY_18	8	+	1.999e-19	1.999e-18	5.51	:VWA1	39	4	0	0	1	0	0	0	30	0	0	0
	19	chr1	1376365	1376683	p001_HEK293T_S1_SVSY_19	8	+	1e-28	1.760e-28	7.18	:VWA1	54	10	1	0	0	11	0	7	10	0	0	0
	20	chr1	1550854	1551205	p001_HEK293T_S1_SVSY_20	4	+	0.000001947	0.000007991	3.43	:MIR2	28	0	0	0	0	0	0	2	12	0	0	0
	21	chr1	1554580	1555009	p001_HEK293T_S1_SVSY_21	4	+	0.0001175	0.0006457	3.32	:MIR2	26	4	0	0	0	0	0	4	12	0	0	0
	22	chr1	2116073	2116834	p001_HEK293T_S1_SVSY_22	5	+	6.31e-24	7.043e-23	4.72	:PRKCE2	60	6	1	0	0	34	0	19	0	0	0	0
	23	chr1	2160462	2160542	p001_HEK293T_S1_SVSY_23	3	+	0.00002754	0.0003226	2.89	:SKI	29	2	1	0	0	0	0	42	193	0	0	0
	24	chr1	2160790	2234422	p001_HEK293T_S1_SVSY_24	12	+	1e-54	2.512e-53	11.5	:SKI	62	2	3	0	0	0	0	55	193	0	0	0
	25	chr1	2230305	2230904	p001_HEK293T_S1_SVSY_25	15	-	0.0000000000000031	0.0000000000000031	14.5	:SKI	71	8	0	0	0	0	0	193	0	0	0	0

Showing 1 to 25 of 1,338,085 entries

Column-wise search (launched by any input)

**Figure S4. Illustration of table view.** Table view is capable of displaying background data clearly and providing several search methods. To be more specific, global search can query input information within entire table. Column specific search, located in the footer of table, can perform search within corresponding column. More important, we designed a variety of advanced search functions for different tables to further assist users to screen out the most valuable elements among the huge information stored in the background database. Users can export data by clicking export buttons under any search conditions for further investigation. Besides, users are able to view detailed information in the genome browser of a specific entry by clicking the genome browser icon at the very left end of each row.

**Table S1. Studies from which the MeT-DB V2.0 core data samples were obtained**

ID	Papa Abbr	Title	Species	Year
1	p001	Comprehensive Analysis of mRNA Methylation Reveals Enrichment in 3'UTRs and near Stop Codons	Human, Mouse	2012
2	p002	Topology of the human and mouse m <sup>6</sup> A RNA methylomes revealed by m <sup>6</sup> A -seq	Human, Mouse	2012
3	p004	RNA-Methylation-Dependent RNA Processing Controls the Speed of the Circadian Clock	Human	2013
4	p005	The fat mass and obesity associated gene (Fto) regulates activity of the dopaminergic midbrain circuitry	Mouse	2013
5	p006	High-Resolution Mapping Reveals a Conserved, Widespread, Dynamic mRNA Methylation Program in Yeast Meiosis	Yeast	2013
6	p007	N6-methyladenosine-dependent regulation of messenger RNA stability	Human	2014
7	p009	Perturbation of m <sup>6</sup> A writers reveals two distinct classes of mRNA methylation at internal and 5' sites	Human, Mouse	2014
8	p010	m <sup>6</sup> A RNA modification controls cell fate transition in mammalian embryonic stem cells	Human, Mouse	2014
9	p011	FTO-dependent demethylation of N6-methyladenosine regulates mRNA splicing and is required for adipogenesis	Mouse	2014
10	p017	Unique features of the m <sup>6</sup> A methylome in Arabidopsis thaliana	Thaliana	2014
11	p019	N6-methyladenosine marks primary microRNAs for processing	Human	2015
12	p020	N6-Adenosine Methylation in MiRNAs	Human	2015
13	p021	m <sup>6</sup> A RNA methylation is regulated by microRNAs and promotes reprogramming to pluripotency	Mouse	2015
14	p022	m <sup>6</sup> A mRNA methylation facilitates resolution of naive pluripotency toward differentiation	Mouse	2015
15	p027	Dynamic m <sup>6</sup> A mRNA methylation directs translational control of heat shock response	Mouse	2015
16	p028	Transcriptome-wide high-throughput deep m <sup>6</sup> A -seq reveals unique differential m <sup>6</sup> A methylation patterns between three organs in Arabidopsis thaliana	Thaliana	2015
17	p032	The m <sup>6</sup> A Methyltransferase METTL3 Promotes Translation in Human Cancer Cells	Human	2016
18	p035	Dynamics of the human and viral m <sup>6</sup> A RNA methylomes during HIV-1 infection of T cells	Human	2016
19	p037	N6-Methyladenosine RNA Modification Regulates Shoot Stem Cell Fate in Arabidopsis	Thaliana	2016
20	p041	N6-methyladenosine of HIV-1 RNA regulates viral infection and HIV-1 Gag protein expression	Human	2016
21	p045	Dynamics of Human and Viral RNA Methylation during Zika Virus Infection	Human, Zika	2016
22	p046	N6-Methyladenosine in Flaviviridae Viral RNA Genomes Regulates Infection	Human	2016
23	p047	m <sup>6</sup> A modulates neuronal functions and sex determination in Drosophila	Drosophila	2016
24	p049	FTO Plays an Oncogenic Role in Acute Myeloid Leukemia as a N 6-Methyladenosine RNA Demethylase	Mouse	2017
25	p055	Genome-wide mapping of 5-hydroxymethyluracil in the eukaryote parasite Leishmania	Zebrafish	2017
26	p056	mRNA N6-methyladenosine methylation of postnatal liver development in pig	Pig	2017

**Table S2. Studies from which the TREW data samples were obtained**

ID	Reference Title	Species	Technic	Regulator Name	Regulator Type	Year
1	The fat mass and obesity associated gene (Fto) regulates activity of the dopaminergic midbrain circuitry	Mouse	MeRIP-seq	FTO	Eraser	2013
3	Perturbation of m <sup>6</sup> A Writers reveals two distinct classes of mRNA methylation at internal and 5' sites	Human, Mouse	MeRIP-seq	WTAP,KIAA1429, METTL3,METTL14	Writer	2014
2	FTO-dependent demethylation of N6-methyladenosine regulates mRNA splicing and is required for adipogenesis	Mouse	MeRIP-seq	FTO	Eraser	2014
4	A METTL3-METTL14 complex mediates mammalian nuclear RNA N6-adenosine methylation	Human	MeRIP-seq, PAR-CLIP	WTAP,METTL3, METTL14	Writer	2014
5	Dynamic m <sup>6</sup> A mRNA methylation directs translational control of heat shock response	Mouse	MeRIP-seq	FTO	Eraser	2015
6	m <sup>6</sup> A mRNA methylation facilitates resolution of naive pluripotency toward differentiation	Mouse	MeRIP-seq	METTL3	Writer	2015
7	N6-methyladenosine-dependent RNA structural switches regulate RNA-protein interactions	Human	PAR-CLIP	METTL3,METTL14, HNRNPC	Writer	2015
8	N6-methyladenosine Modulates Messenger RNA Translation Efficiency	Human	PAR-CLIP	YTHDF1	Reader	2015
9	FTO Plays an Oncogenic Role in Acute Myeloid Leukemia as a N6-Methyladenosine RNA Demethylase	Human	MeRIP-seq	FTO	Eraser	2016
10	Structural basis for selective binding of m <sup>6</sup> A RNA by the YTHDC1 YTH domain	Human	PAR-CLIP	YTHDC1	Reader	2016